



# Predicting the Inflow Distortion Tone Noise of the NASA Glenn Advanced Noise Control Fan With a Combined Quadrupole-Dipole Model

*L. Danielle Koch*  
*Glenn Research Center, Cleveland, Ohio*

## NASA STI Program . . . in Profile

Since its founding, NASA has been dedicated to the advancement of aeronautics and space science. The NASA Scientific and Technical Information (STI) program plays a key part in helping NASA maintain this important role.

The NASA STI Program operates under the auspices of the Agency Chief Information Officer. It collects, organizes, provides for archiving, and disseminates NASA's STI. The NASA STI program provides access to the NASA Aeronautics and Space Database and its public interface, the NASA Technical Reports Server, thus providing one of the largest collections of aeronautical and space science STI in the world. Results are published in both non-NASA channels and by NASA in the NASA STI Report Series, which includes the following report types:

- **TECHNICAL PUBLICATION.** Reports of completed research or a major significant phase of research that present the results of NASA programs and include extensive data or theoretical analysis. Includes compilations of significant scientific and technical data and information deemed to be of continuing reference value. NASA counterpart of peer-reviewed formal professional papers but has less stringent limitations on manuscript length and extent of graphic presentations.
- **TECHNICAL MEMORANDUM.** Scientific and technical findings that are preliminary or of specialized interest, e.g., quick release reports, working papers, and bibliographies that contain minimal annotation. Does not contain extensive analysis.
- **CONTRACTOR REPORT.** Scientific and technical findings by NASA-sponsored contractors and grantees.

- **CONFERENCE PUBLICATION.** Collected papers from scientific and technical conferences, symposia, seminars, or other meetings sponsored or cosponsored by NASA.
- **SPECIAL PUBLICATION.** Scientific, technical, or historical information from NASA programs, projects, and missions, often concerned with subjects having substantial public interest.
- **TECHNICAL TRANSLATION.** English-language translations of foreign scientific and technical material pertinent to NASA's mission.

Specialized services also include creating custom thesauri, building customized databases, organizing and publishing research results.

For more information about the NASA STI program, see the following:

- Access the NASA STI program home page at <http://www.sti.nasa.gov>
- E-mail your question to [help@sti.nasa.gov](mailto:help@sti.nasa.gov)
- Fax your question to the NASA STI Information Desk at 443-757-5803
- Phone the NASA STI Information Desk at 443-757-5802
- Write to:  
STI Information Desk  
NASA Center for AeroSpace Information  
7115 Standard Drive  
Hanover, MD 21076-1320



# Predicting the Inflow Distortion Tone Noise of the NASA Glenn Advanced Noise Control Fan With a Combined Quadrupole-Dipole Model

*L. Danielle Koch*  
*Glenn Research Center, Cleveland, Ohio*

Prepared for the  
18th Aeroacoustics Conference  
cosponsored by the American Institute of Aeronautics and Astronautics and  
the Confederation of European Aerospace Societies  
Colorado Springs, Colorado, June 4–6, 2012

National Aeronautics and  
Space Administration

Glenn Research Center  
Cleveland, Ohio 44135

## Acknowledgments

I would like to thank Marvin Goldstein for his guidance in understanding the details of the theoretical model. I also appreciate the efforts of the AeroAcoustic Propulsion Laboratory staff in obtaining the experimental data, Gary Podboy and Dan Sutliff for obtaining the wake measurements, and Daniel L. Tweedt for providing the computational fluid dynamics analysis. Funding for this research has been provided by the Subsonic Fixed Wing Project which is a part of NASA's Fundamental Aeronautics Program.

This work was sponsored by the Fundamental Aeronautics Program  
at the NASA Glenn Research Center.

*Level of Review:* This material has been technically reviewed by technical management.

Available from

NASA Center for Aerospace Information  
7115 Standard Drive  
Hanover, MD 21076-1320

National Technical Information Service  
5301 Shawnee Road  
Alexandria, VA 22312

Available electronically at <http://www.sti.nasa.gov>

# Predicting the Inflow Distortion Tone Noise of the NASA Glenn Advanced Noise Control Fan With a Combined Quadrupole-Dipole Model

L. Danielle Koch  
National Aeronautics and Space Administration  
Glenn Research Center  
Cleveland, Ohio 44135

## Abstract

A combined quadrupole-dipole model of fan inflow distortion tone noise has been extended to calculate tone sound power levels generated by obstructions arranged in circumferentially asymmetric locations upstream of a rotor. Trends in calculated sound power level agreed well with measurements from tests conducted in 2007 in the NASA Glenn Advanced Noise Control Fan. Calculated values of sound power levels radiated upstream were demonstrated to be sensitive to the accuracy of the modeled wakes from the cylindrical rods that were placed upstream of the fan to distort the inflow. Results indicate a continued need to obtain accurate aerodynamic predictions and measurements at the fan inlet plane as engineers work towards developing fan inflow distortion tone noise prediction tools.

## Nomenclature

$A_{q,s}$	Fourier coefficient of axial distortion velocity
$a_q$	circumferential Fourier coefficients of the axial distortion velocity profile
$AR$	aspect ratio
$B$	number of rotor blades
$b$	blade height
$c_0$	speed of sound
$c$	rotor chord length
$D$	compressibility correction factor defined by Equation (8)
$d_s$	radial Fourier coefficients of axial distortion velocity profile defined by Equation (2)
$H_{p,q,s}$	complex conjugate of $H_{p,q,s}$
$\bar{H}_{p,q,s}$	complex conjugate of $H_{p,q,s}$
$i$	$\sqrt{-1}$
$I$	ratio of maximum distortion velocity to mean axial velocity $U$ defined by Equation (3)
$K_{p,q,s}$	dimensionless circumferential location of inlet obstructions
$J_j$	dimensionless circumferential location of inlet obstructions
$M$	axial Mach number, $U/c_0$
$M_r$	relative Mach number, $U_r/c_0$
$M_t$	rotor tip Mach number, $U_t/c_0$
$N$	number of upstream vanes or struts, integer 1, 2, ...
$\mathcal{P}_p$	total acoustic power radiated upstream in the $p^{\text{th}}$ harmonic of the blade passing frequency
$\bar{R}$	mean radius
$S(\sigma_q)$	Sears function, defined in Equation (6)
$U$	axial flow velocity
$Ur$	relative velocity, $-\sqrt{U_t + U^2}$
$U_t$	cascade (rotor) velocity
$y_i$	coordinates of source point

$w_i$	phase-locked rotor velocity field relative velocity field
$\beta$	$\sqrt{1 - M^2}$
$\beta_r$	$\sqrt{1 - M_r^2}$
$\Delta$	interblade spacing
$\delta$	circumferential distance, $B\Delta$
$\delta_{i,j}$	Kronecker delta
$\Theta_{p,q,s}$	defined by Equation (4)
$\theta$	work coefficient, $-\Delta w_2 / U_t$
$\rho_0$	background density
$\sigma'$	half-width of Gaussian/step profile
$\sigma_q$	reduced frequency, $\frac{q\Omega c}{2U_r}$
$\tilde{\sigma}$	dimensionless radial height of axial distortion velocity profile
$\psi$	defined by Equation (5)
$\Omega$	shaft rotational frequency, $\frac{2\pi U_t}{\delta}$

#### Subscripts

$i, j, k$	integer 1, 2, 3, ...
$s$	integer 0, 1, 2, ...
$p, q$	integer, 0, $\pm 1$ , $\pm 2$ , ...

## Introduction

A combined quadrupole-dipole analytic model of fan inflow distortion tone noise was published by Goldstein, Dittmar, and Gelder in 1974 (Ref. 1). Their intention was to predict the upstream-radiated tone noise from a fan with a high-subsonic rotor tip speed that was ingesting flow distorted by the presence of uniformly spaced upstream struts. They chose to retain the quadrupole source term in a generalized version of the Ffowcs Williams and Hawkings (Refs. 2 and 3) formulation based on a previous suggestion of Morfey (Ref. 4), whose simplified analysis suggested that sound generated by the quadrupole term may be equal to or greater than the sound generated by a dipole term for axial Mach numbers of the inflow as low as 0.25. Indeed, upon examining the final form of the equations of the combined quadrupole-dipole model, Goldstein et al. noted that the dipole term was independent of the work coefficient of the fan, but that the quadrupole term would be greater than the dipole term for highly-loaded, low-solidity fans. A limited amount of experimental data accompanied the original derivation in Reference 1.

The current paper describes an extension of the theory presented by Goldstein, et al. (Ref. 1). The original theory has been extended so that tone sound power levels can be calculated when obstructions are placed at circumferentially asymmetric locations upstream of the rotor to distort the inflow. A computer code called GDGK has been written based on the theory of Goldstein, Dittmar, Gelder extended and programmed by Koch. Computed results are compared here against data from a test conducted with the NASA Glenn Advanced Noise Control Fan (ANCF) in 2007. Data from the ANCF experiments is considered to be a partial validation of this model, as the quadrupole generation mechanism was not a dominant component of the inflow distortion tones for this low-speed, lightly loaded fan.

## Prediction Method

Goldstein et al. presented a derivation of the following equations to estimate sound power of the blade passing frequency (BPF) harmonic tones radiated upstream of a fan ingesting distorted inflow (see pp. 12, and 25 to 28 of Ref. 1). Many assumptions were made to arrive at these equations; such as modeling the

fan duct as an unrolled rectangular duct, modeling the rotor potential flow field as a line of free vortices, and using a Gaussian function to model the wakes of the upstream stators or vanes. These original equations were incorporated into the first version of the computer code GDGK.v1. The first term of Equation (4) is associated with the quadrupole mechanism, and the second term in Equation (4) is associated with the dipole mechanism.

$$\frac{P_p}{\rho_0 c_0^3 B b \Delta} = \frac{(MM_t)^2 p M_t}{4} \sum (1 + \delta_{s,0}) \frac{|\Theta_{p,q,s}|^2 |A_{q,s}|^2}{(M_t p + MK_{p,q,s})^2 K_{p,q,s}} \quad (1)$$

all  $q$  and all  $s \geq 0$  with

$$p^2 M_t^2 > \beta^2 \left[ \left( p - \frac{q}{B} \right)^2 + \left( \frac{\sigma'}{2b} \right)^2 \right]$$

$$H_{p,q,s} = \frac{\left( p - \frac{q}{B} \right) \beta^2 - iD(MM_t p + K_{p,q,s})}{p\beta_r - iK_{p,q,s}} \quad (2)$$

$$K_{p,q,s} = \sqrt{p^2 M_t^2 - \beta^2 \left[ \left( p - \frac{q}{B} \right)^2 + \left( \frac{s\Delta}{2b} \right)^2 \right]} \quad (3)$$

$$\Theta_{p,q,s} \equiv -\theta \bar{H}_{p,q,s} (MM_t p + K_{p,q,s}) + i\psi S(\sigma_q) \left[ \frac{M(pB - q)\beta^2}{B} - M_t (MM_t p + K_{p,q,s}) \right] \quad (4)$$

$$\psi = \frac{1}{2M_r} \left( \frac{c}{\Delta} \right) \left[ \frac{2\pi AR}{AR + 2 \left( \frac{AR + 4}{AR + 2} \right)} \right] \quad (5)$$

$$S(\sigma_q) = \frac{\exp(-i\sigma_q) \left[ 1 - \frac{\pi^2}{2(1 + 2\pi|\sigma_q|)} \right]}{\sqrt{1 + 2\pi|\sigma_q|}} \quad (6)$$

$$\sigma_q = \frac{q\pi M_t}{BM_r} \left( \frac{c}{\Delta} \right) \quad (7)$$

$$D \equiv \frac{\beta_r + iMM_t}{\beta^2} \quad (8)$$

In order to evaluate Equation (1), it is necessary to determine values for  $A_{q,s}$ , the Fourier coefficients of the axial distortion velocity profile. Goldstein, et al. described one way in Reference 1 that is partially repeated here. If you assume

$$A_{q,s} = I a_q d_s$$

$$a_q = \frac{1}{\delta} \int_0^{\delta} e^{-2\pi i q y_2 / \delta} f(y_2) dy_2 \quad (9)$$

When the flow distortion is represented by  $N$  uniformly spaced Gaussian profiles in the circumferential direction such that

$$f(y_2) = \exp \left[ \frac{-\left(\frac{y_2}{\delta} - \frac{1+2j}{2N}\right)^2}{(\sigma')^2} \right] \left\{ \begin{array}{l} \frac{j\delta}{N} < y_2 < \frac{(j+1)\delta}{N} \\ \text{for } j = 0, 1, \dots, N \end{array} \right\} \quad (10)$$

$$a_q = \sqrt{\pi} N \sigma' e^{-\frac{i\pi q}{N}} e^{-\pi^2 q^2 (\sigma')^2} \operatorname{Re} \left[ \operatorname{erf} \left( \frac{1}{2N\sigma'} + \pi i q \sigma' \right) \right] \text{ for } q = 0, \pm N, \pm 2N, \dots \quad (11)$$

$$a_q = 0 \text{ for } q \neq 0, \pm N, \pm 2N, \dots \quad (12)$$

In the radial direction,

$$d_s = \delta_{s,0} \text{ if the flow distortion is uniform in the radial direction, or} \quad (13)$$

$$d_s = \frac{2(-1)^s}{\pi s(1 + \delta_{s,0})} \sin(\pi s \tilde{\sigma}) \text{ if the flow distortion is a square wave concentrated around the tip region} \quad (14)$$

However, sound power level can also be calculated for circumferentially asymmetric obstructions in the inlet duct if one chooses a more general form of Equation (10), resulting in a slightly different form for  $a_q$ , the circumferential Fourier coefficients of axial distortion velocity profile, where  $J_j$  is the dimensionless circumferential location of the upstream obstructions in the flow.

$$f(y_2) = \exp \left[ \frac{-\left(\frac{y_2}{\delta} - J_j\right)^2}{(\sigma')^2} \right] \left\{ \begin{array}{l} 0 \leq \frac{y_2}{\delta} \leq 1 \\ \text{for } j = 0, 1, 2, \dots, N \end{array} \right\} \quad (15)$$

$$a_q = \frac{\sigma' \sqrt{\pi}}{2} e^{-2\pi i q J_j} e^{-(\pi q \sigma')^2} \sum_{j \geq 0} \left[ \operatorname{erf} \left( \frac{J_j}{\sigma'} - i\pi q \sigma' \right) + \operatorname{erf} \left( \frac{1 - J_j + i\pi q \sigma'^2}{\sigma'} \right) \right] \text{ for all } q \quad (16)$$

This model was incorporated into the second version of the computer code, GDGK.v2. Figure 1 shows the notional differences between symmetric and asymmetrically arranged Gaussian curves that can be used to model the wakes. In the final form of the sound power level calculations, wake depth, width, radial extent, and circumferential placement are set using variables  $I$ ,  $\sigma'$ ,  $\tilde{\sigma}$ , and  $J_j$ , respectively.

Predictions from the new GDGK code were generated for the 51-cm fan studied in Reference 1. Figure 2 shows the original published results and the new calculations from the GDGK.v1 and GDGK.v2 codes. Generally, there is good agreement between the original and new predictions. Results from GDGK.v1 and GDGK.v2 were identical. Some of the differences between the original and new predictions are attributed to uncertainties in the input values for the calculations. While the original reports included values for most of the input quantities, the experimental value for fan inlet temperature was not presented which is needed to determine fan corrected speed and inflow variables. So for the new

GDGK predictions, it was assumed that the rotor speed settings were 10,666, 9,333, and 8,000 rpm; and that density was  $0.800 \text{ kg/m}^3$  and acoustic speed was 336 m/s. Also, since sound power levels were not published in tabular form, there may be some errors in the historical values presented in Figure 2, which were determined by a manual inspection of the original plot.

## Experiment

A fan inlet distortion experiment was conducted in 2007 using the NASA Glenn Advanced Noise Control Fan that is housed within AeroAcoustic Propulsion Laboratory (AAPL), as shown in Figure 3. The ANCF is 1.2 m (48 in.) in diameter and the centerline of the fan is 3.0 m (10 ft) above the floor. For both tests, no stator vanes were installed downstream of the rotor. The rotor had 16 blades set at a  $28^\circ$  pitch angle for all test conditions.

An Inflow Control Device (ICD) was used to condition the flow entering the fan, removing large-scale turbulence and ground vortices. The inlet plane was located 0.920 m (36.2 in.) or approximately 0.750 L/D ahead of the leading edge of the fan at the tip location. The exhaust plane was located 1.20 m (45.4 in.) or approximately 1.0 L/D downstream of the trailing edge of the fan at the tip location. Downstream of the test section, the centerbody diameter increases to 0.710 m (24.0 in.) to mimic a nozzle area contraction, yielding a hub-to-tip ratio of,  $\sigma = 0.500$ . The hub diameter at the rotor leading edge was 0.460 m (18.0 in.), yielding a hub-to-tip ratio of,  $\sigma = 0.375$ .

The inflow to the rotor was distorted by installing smooth cylindrical rods upstream of the rotor, as shown in Figure 4. The rods were 1.27 cm (0.500 in.) in diameter and were 31.8 cm (12.5 in.) long, resulting in a 6.35 cm (2.50 in.) gap between the bottom of the rods and the rotor hub. The centerline of the rods was 14.3 cm (5.63 in.) upstream of the rotor leading edge at the tip, or approximately one rotor chord length upstream. Data were recorded at three speed settings: 1400, 1800, and 2000 rpm. Four distortion patterns were tested in the 2007 experiment, as shown in Figure 5. A 30-rod mounting ring allowed rods to be placed at circumferential locations separated by increments of  $12^\circ$ . The experiment is described in more detail in References 5 to 7.

Two 15-microphone arrays were used to record the farfield sound distribution from the ANCF. Farfield microphone measurements were acquired synchronously with shaft speed at a rate of 256 samples per revolution, which allow for processing up to the 128<sup>th</sup> harmonic of the shaft frequency, or equivalently, up to the 8<sup>th</sup> harmonic of the blade passing frequency for this test (Ref. 8).

In-duct acoustic pressure measurements upstream and downstream of the rotor were acquired with the Rotating Rake system. The Rotating Rake system is a continuously rotating radial microphone rake that was inserted into the duct, at either the inlet entrance or exhaust exit plane. The system utilizes annular duct spinning mode theory and Doppler-shift physics to separate circumferential modes and the cylindrical wave equation solution to reduce the radial modes. It provides a complete map of the acoustic duct modal magnitudes and phases present in the fan duct. For these experiments the data were processed for the first two harmonics of blade passing frequency (Ref. 9).

The axial and tangential velocities downstream of a cylindrical rod were experimentally measured with a two-component hotwire probe. The probe was installed in radial and circumferential actuators mounted to the outside of the duct. The maximum traverse span for the circumferential actuator was  $30^\circ$ . Data were recorded at four radial locations: 0.330 m (13.5 in.), 0.419 m (16.5 in.), 0.508 m (20.0 in.), and 0.570 m (23.5 in.).

## Comparison of Calculated and Measured Sound Power Levels

Calculated values of the sound power levels radiated upstream were generated using the GDGK.v2 code for the four configurations tested in the ANCF during the 2007 inlet distortion test. Figures 6 through 8 show the computed and measured wakes from the rods, which were used to determine the wake width and depth parameters needed for the sound power level calculation. Figure 6 show the normalized

axial velocity distribution at a radial station near the tip of the rotor,  $\bar{R} = 0.591$  m (23.25 in.), which was the value used to determine the length of the unrolled rectangular duct modeling the fan, taken here to be the radius at 5 percent of the blade span from the tip. Figure 7 shows that the calculated wake depth decreases and the calculated wake width slightly increases as the flow approaches the inlet to the fan. TSWIFT, a Reynolds-averaged Navier Stokes solver was used to generate the mean flow predictions. Figure 8 shows predicted and measured distribution of the normalized axial velocity at a position slightly closer to the rotor tip ( $\bar{R} = 0.597$  m (23.5 in.) and at an axial location of  $X = -0.113$  m (-4.45 in.). Comparisons indicate that the measured wake was significantly wider and shallower than the predicted wake.

Figures 9 show plots of calculated sound power levels radiated upstream as a function of blade passing frequency (BPF) harmonic. The measurements on these plots are from the inlet duct farfield microphone array. Using non-dimensional wake width ( $\sigma' = 0.0039$ ) and depth ( $I = 0.299$ ) parameters based on the computational fluid dynamics (CFD) solution at  $X = 0.0254$  m (-1.00 in.), calculated sound power levels were greater than measurements, showing a more gradual decrease in amplitude for the higher harmonics than was indicated by the experiment. However, by choosing parameters to model a wider, shallower wake ( $\sigma' = 0.0060$ ,  $I = 0.080$ ) at the fan inlet, which is consistent with the measured trends, better agreement between calculated and measured sound power level trends can be achieved. Experimental data in the wake of the rods at this axial location near the rotor leading edge were not available.

One may also hypothesize, given the results shown in Figure 9, that had the rods been placed closer to the fan leading edge, the overall levels of tone sound power levels could be significantly increased. Deeper and narrower wakes interacting with the rotor may raise the sound power levels of the higher harmonics. This may be of particular concern to aircraft and spacecraft ventilation system designers who may be faced with installing fans in convoluted ducts or near other system obstructions that can significantly distort the fan inflow. Alternately, aircraft engine designers will need accurate aerodynamic predictions and measurements near the fan inlet in order to conduct useful inlet duct acoustic design studies.

Figure 10 through 12 compare the calculated and measured sound power levels for the circumferential and radial modes in the inlet duct for the 1 BPF and 2 BPF tones for the four tested configurations at 2000 rpm. The measurements were obtained from the Rotating Rake installed in the inlet to the fan. The algorithm used to process the Rotating Rake microphone signals is based on an annular duct model. The reader is reminded that the sound power level calculations are based on an unrolled rectangular duct model. These modeling differences result in the differences between the sets of propagating modes. Figures 10 through 12 assume a wide, shallow wake ( $\sigma' = 0.006$ ,  $I = 0.08$ ) at the fan inlet. There was generally good agreement between the measured and calculated trends.

Finally, comparison between the measured and calculated sound power levels of the fundamental tone for all three tested speeds and all rod configurations are shown in Figure 13. The green bars indicate the sound power levels computed by the combination of the dipole and quadrupole terms. The sound power levels of the dipole term were computed, as well as the sound power levels of the quadrupole terms, which also appear on Figure 13. The reader is reminded that when the quadrupole and dipole terms are combined, cancellation is possible. The quadrupole mechanism did not contribute significantly to the generation of the blade passing tones since the work coefficient parameter,  $\theta$ , for this fan was small ( $\theta = 0.04$ ). The sound power level calculated from the quadrupole term did increase as fan speed increased. In general, the variation of the sound power level of the fundamental tone with speed was small and agreement between measured and calculated trends was good. The greatest differences between measured and calculated sound power levels are observed for all speeds of Configuration 3, warranting further study. Wake parameters were held constant for all the calculated results in Figure 13 ( $\sigma' = 0.006$ ,  $I = 0.08$ ).

## Conclusion

A combined quadrupole-dipole model of inflow distortion tone noise, derived and initially validated by Goldstein, Dittmar, and Gelder in 1974 currently serves as the theoretical basis for a new Fortran 90 computer code, GDGK. The first version of the code, GDGK.v1 embodies the original theory and can be used to generate estimates of the tone sound power radiated upstream of a fan ingesting distorted inflow. In this version of the code, it is assumed that multiple obstructions in the inlet are equally spaced in the circumferential direction. Good agreement was shown between calculations from the GDGK.v1 code and the experimental data published in the original report.

The second version of the code, GDGK.v2 embodies an extension of the original theory. By representing the Fourier coefficients of the axial distortion velocity profile in a more general form, tone sound power level estimates can be generated when the obstructions in the fan inlet duct are placed in circumferentially asymmetric locations. GDGK.v2 calculations for the circumferentially asymmetric inlet duct obstructions were compared well against data from the 2007 ANCF inlet distortion experiments. Results indicated that calculated sound power levels were sensitive to the accuracy of the modeled wake.

## References

1. Goldstein, M. E., Dittmar, J. H. and Gelder, T. F., "Combined Quadrupole-Dipole Model for Inlet Flow Distortion Noise from a Subsonic Fan," NASA TN-D-7676, 1974.
2. Ffowes Williams, J. E., Hawkings, D. L., "Theory Relating to the Noise of Rotating Machinery," *Journal of Sound and Vibration*, 10(1), July 1969, pp 10-21.
3. Goldstein, Marvin E.: *Aeroacoustics*. NASA SP-346, 1974, section 4.3.1.
4. Morfey, C. L., *Tone Radiation From an Isolated Subsonic Rotor*, *Journal of the Acoustical Society of America*, 49(5), 1971, pp. 1690-1692.
5. Koch, L. D., "An Experimental Study of Fan Inflow Distortion Tone Noise," NASA/TM—2010-215844, 2010.
6. Koch, L. D., "Predicted and Measured Modal Sound Power Levels for a Fan Ingesting Distorted Inflow," AIAA-2010-3715, 2010.
7. Koch, L. D., "Validation of the Predicted Circumferential and Radial Mode Sound Power Levels in the Inlet and Exhaust Ducts of a Fan Ingesting Distorted Inflow," NASA/TM—2012-217253, 2011.
8. Loew, R. A., Lauer, J. T., McAllister, J. and Sutliff, D. L., "The Advanced Noise Control Fan," NASA/TM—2006-214368, 2006.
9. Sutliff, D. L., "Rotating Rake Turbofan Duct Mode Measurement System," NASA/TM—2005-213828, 2005.

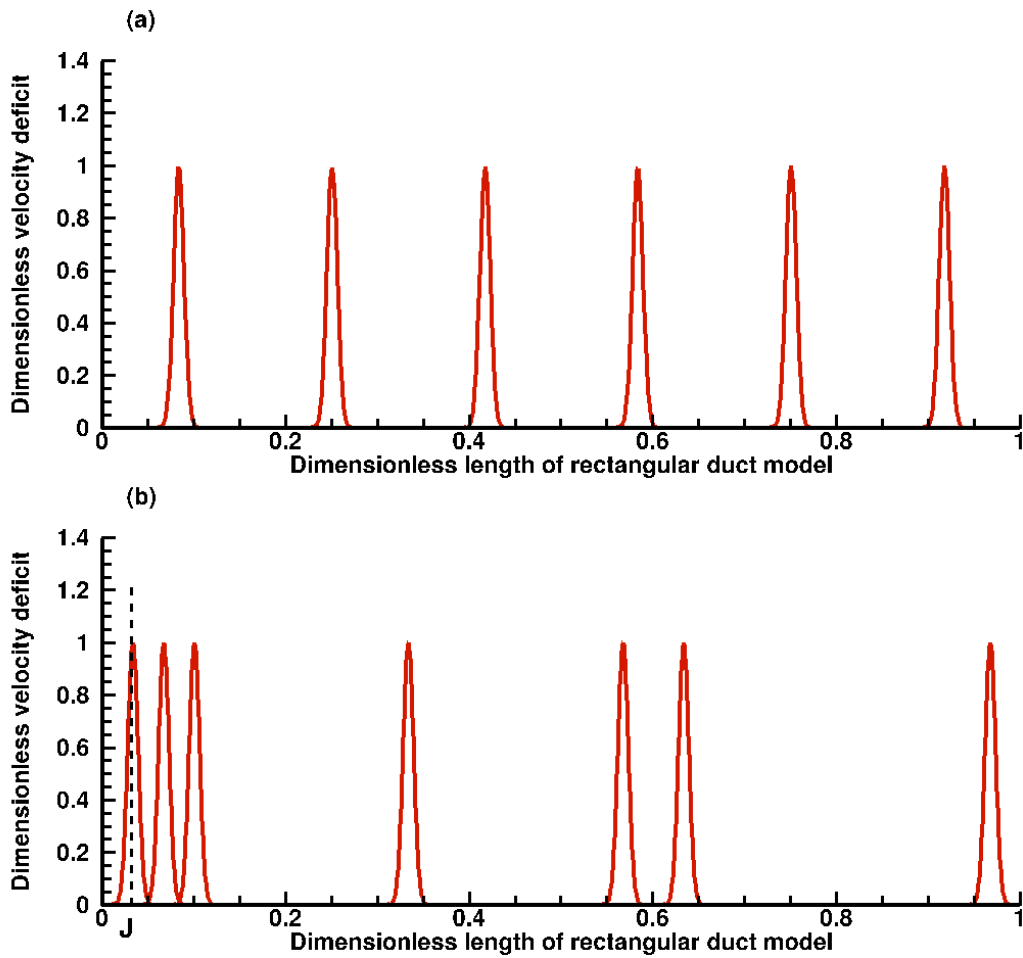


Figure 1.—Notional Gaussian functions used to model wakes from circumferentially (a) symmetric and (b) asymmetric arrangements of upstream struts or vanes that can distort the flow entering a fan. The center location for the wakes depicted in (b) are represented in Equation (15) and (16) by variable  $J_j$ .

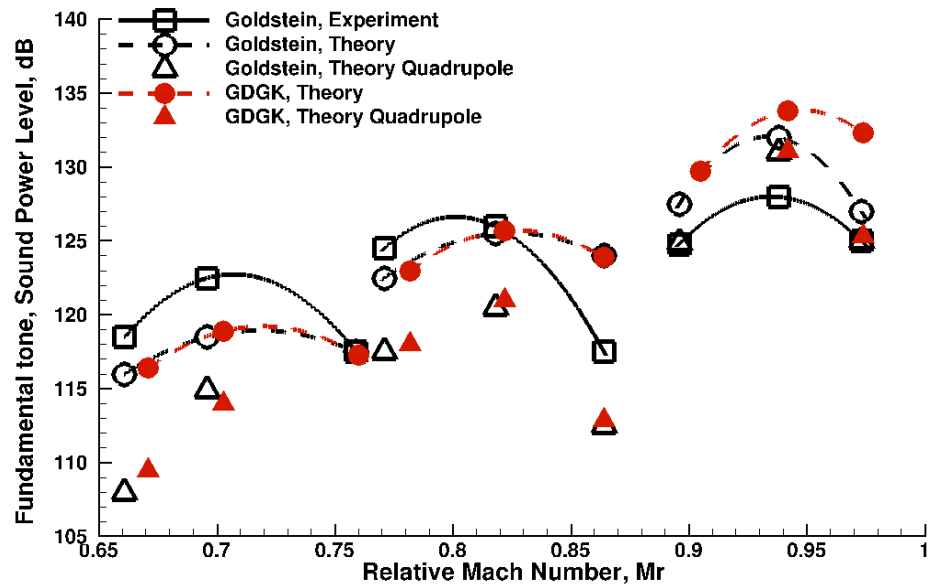


Figure 2.—Predicted and measured sound power levels of the fundamental tone of a 51-cm model fan. Predictions from the GDGK codes are compared to predictions and experimental data originally published by Goldstein et al., Reference 1. Calculated results from GDGK.v1 and GDGK.v2 were identical.

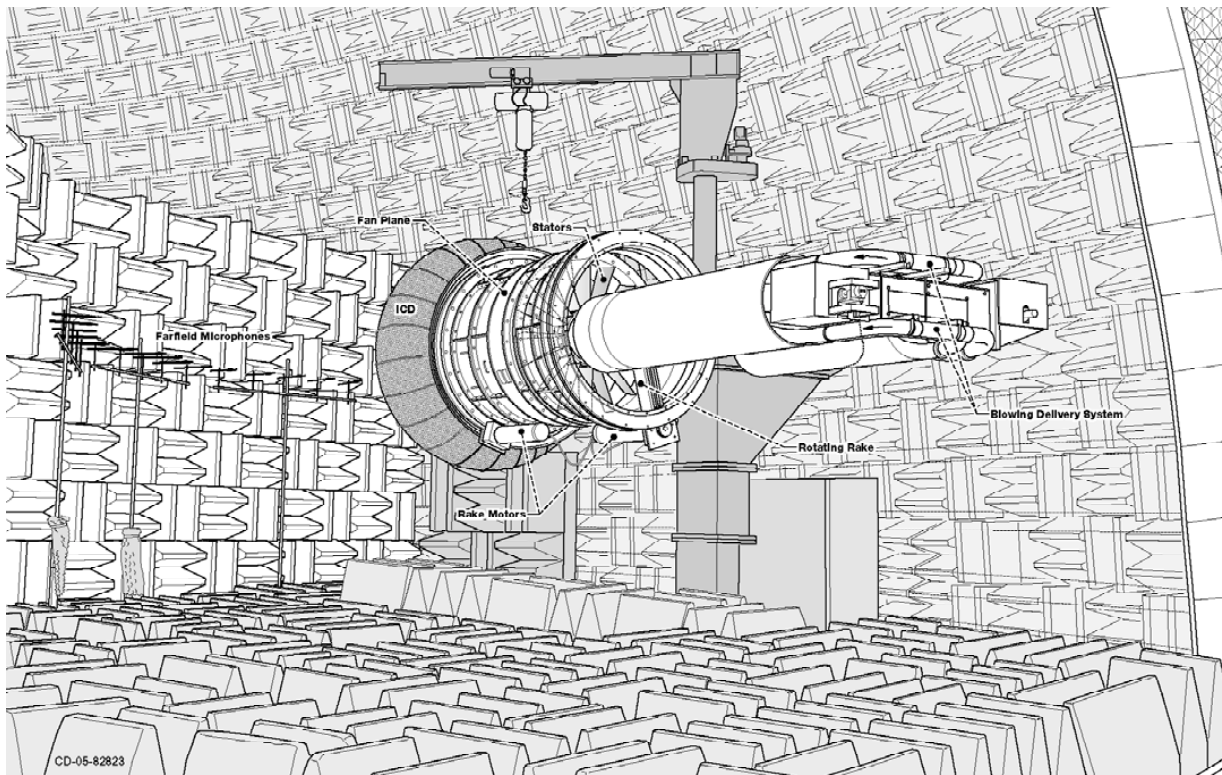


Figure 3.—The Advanced Noise Control Fan in the NASA Glenn AeroAcoustic Propulsion Lab.

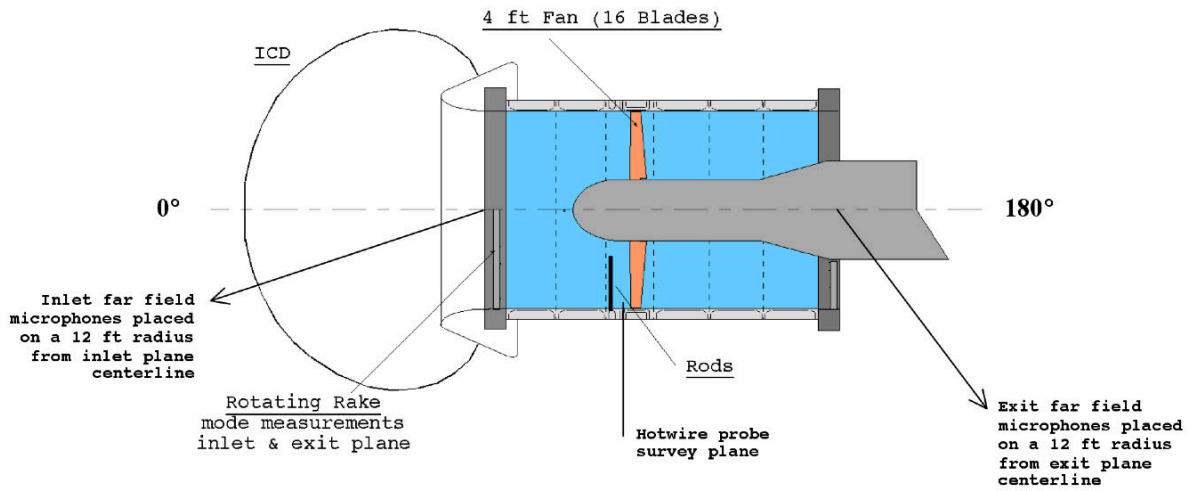


Figure 4.—Cross-sectional diagram of Advanced Noise Control Fan for the inlet distortion tests.

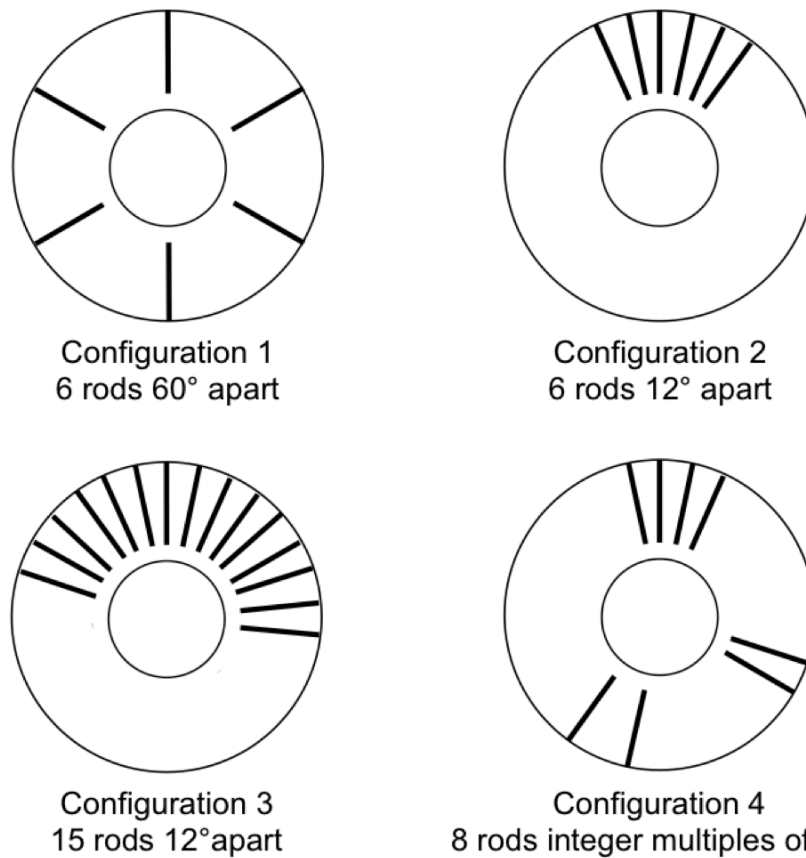


Figure 5.—Circumferential locations of inlet distortion rods tested in 2007 in the ANCF at NASA Glenn.

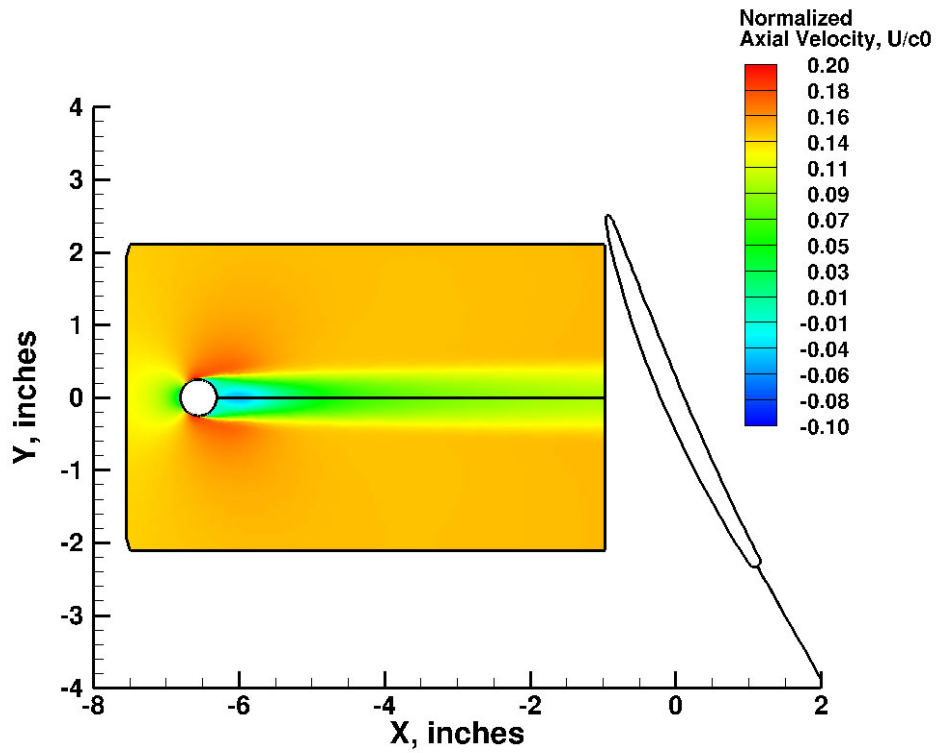


Figure 6.—Contours of normalized axial velocity,  $U/c_0$ , in the wake of a cylindrical rod from TSWIFT, a computational fluid dynamics solver.

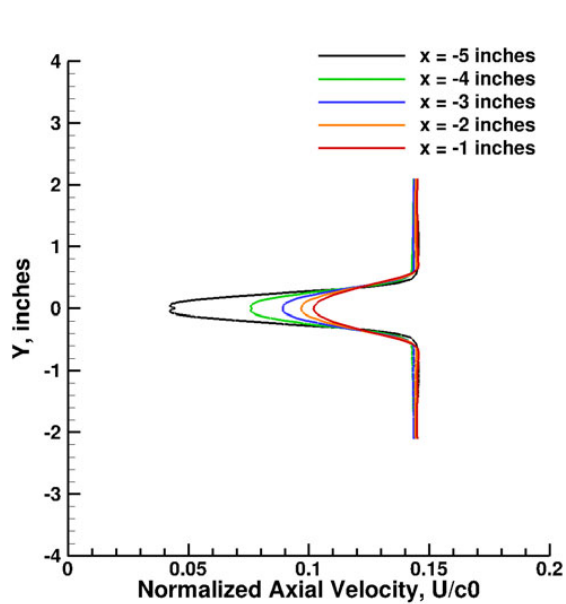


Figure 7.—Predicted wakes at five axial locations at radius  $R = 0.5906$  m (23.25 in) and a rotor speed of 2000 rpm.

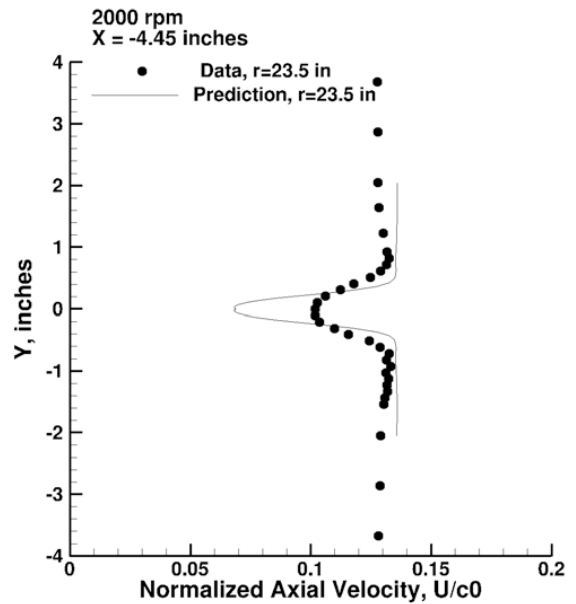


Figure 8.—Predicted and measured wake at radius  $R = 0.597$  m (23.50 in) and axial location  $X = -0.113$  m (-4.45 in).

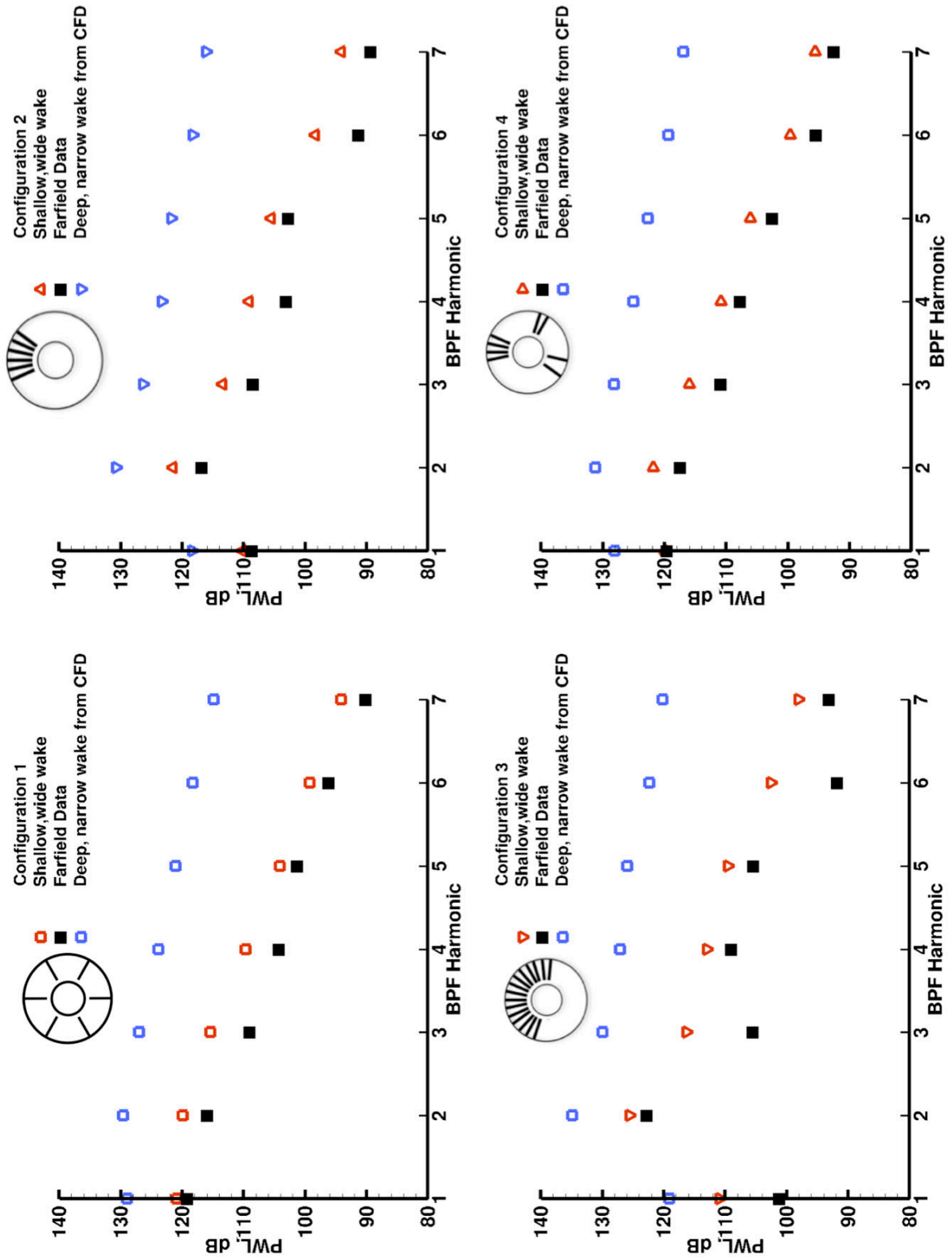


Figure 9.—Calculations of the sound power levels of the blade passing frequency harmonics from the GDGK.v2 code compared with measured far field sound power levels in the inlet region of the NASA Glenn Advanced Noise Control Fan (ANCF), 2000 rpm.

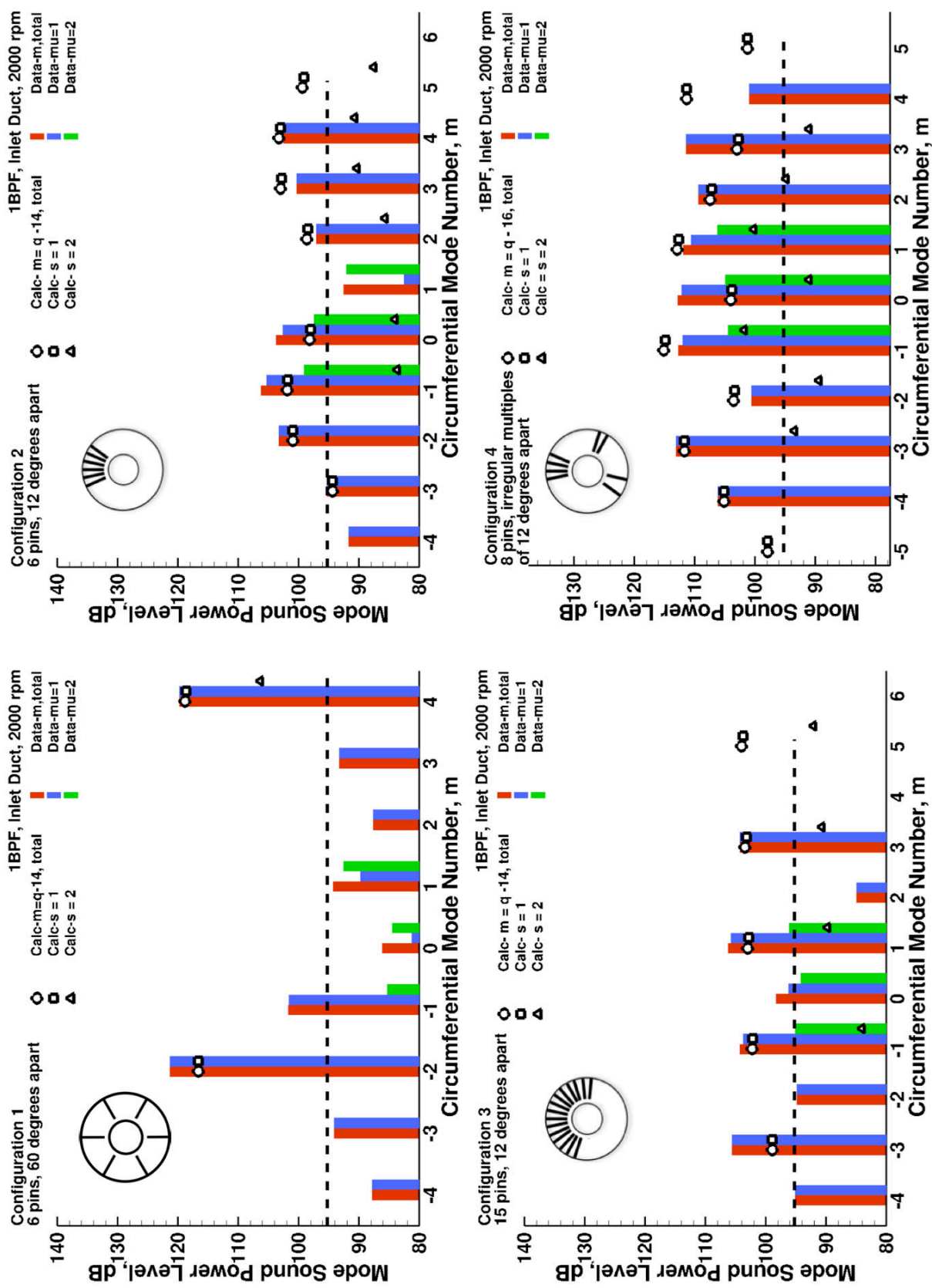
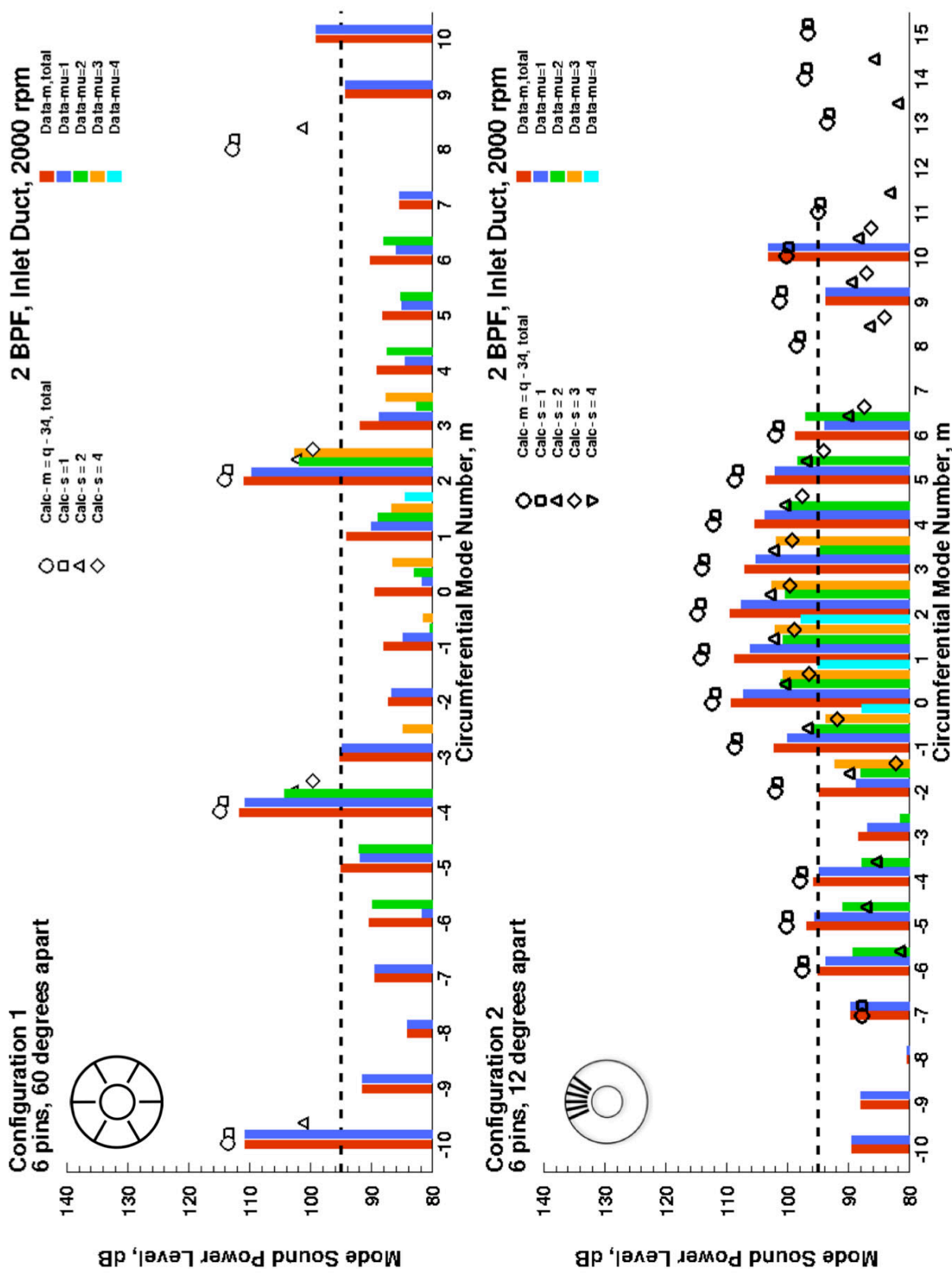


Figure 10.—Calculated ( $P_{1,q,s}$ ) and measured ( $P_{1,m,t}$ ) in-duct circumferential and radial sound power levels for the inlet duct, 1 BPF, 2000 rpm. Horizontal dashed line indicates noise floor for the data set. Measurements were obtained with the ANCF Rotating Rake.



(a) (b)

Figure 11.—Calculated ( $P_{2,q,s}$ ) and measured ( $P_{2,m,\mu}$ ) in-duct circumferential and radial sound power levels for the inlet duct, 2 BPF, 2000 rpm. Horizontal dashed line indicates noise floor for the data set. Measurements were obtained with the ANCF Rotating Rake.

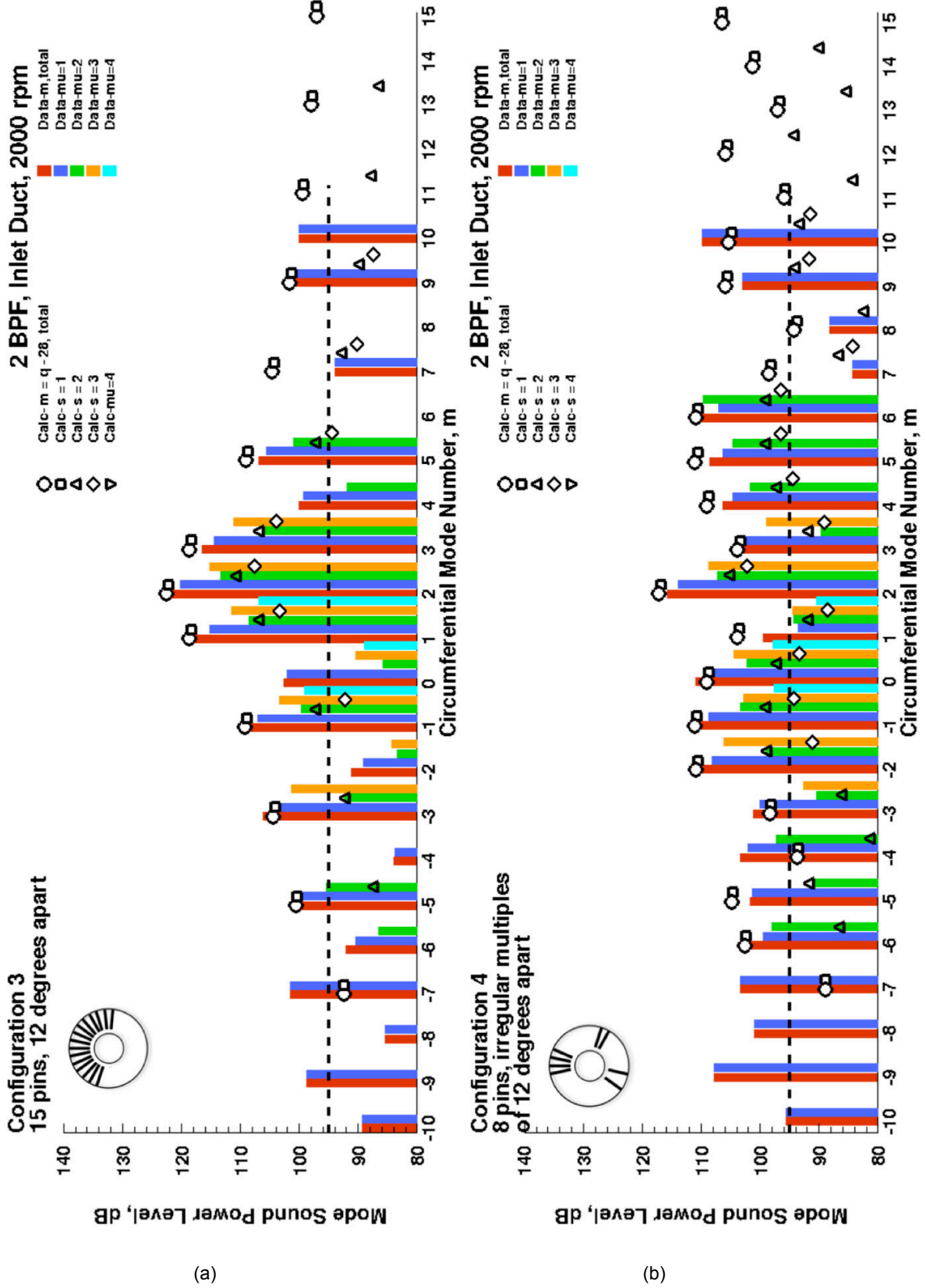


Figure 12.—Calculated ( $P_{2,q,s}$ ) and measured ( $P_{2,m,\mu}$ ) in-duct circumferential and radial sound power levels for the inlet duct, 2 BPF, 2000 rpm. Horizontal dashed line indicates noise floor for the data set. Measurements were obtained with the ANCF Rotating Rake.

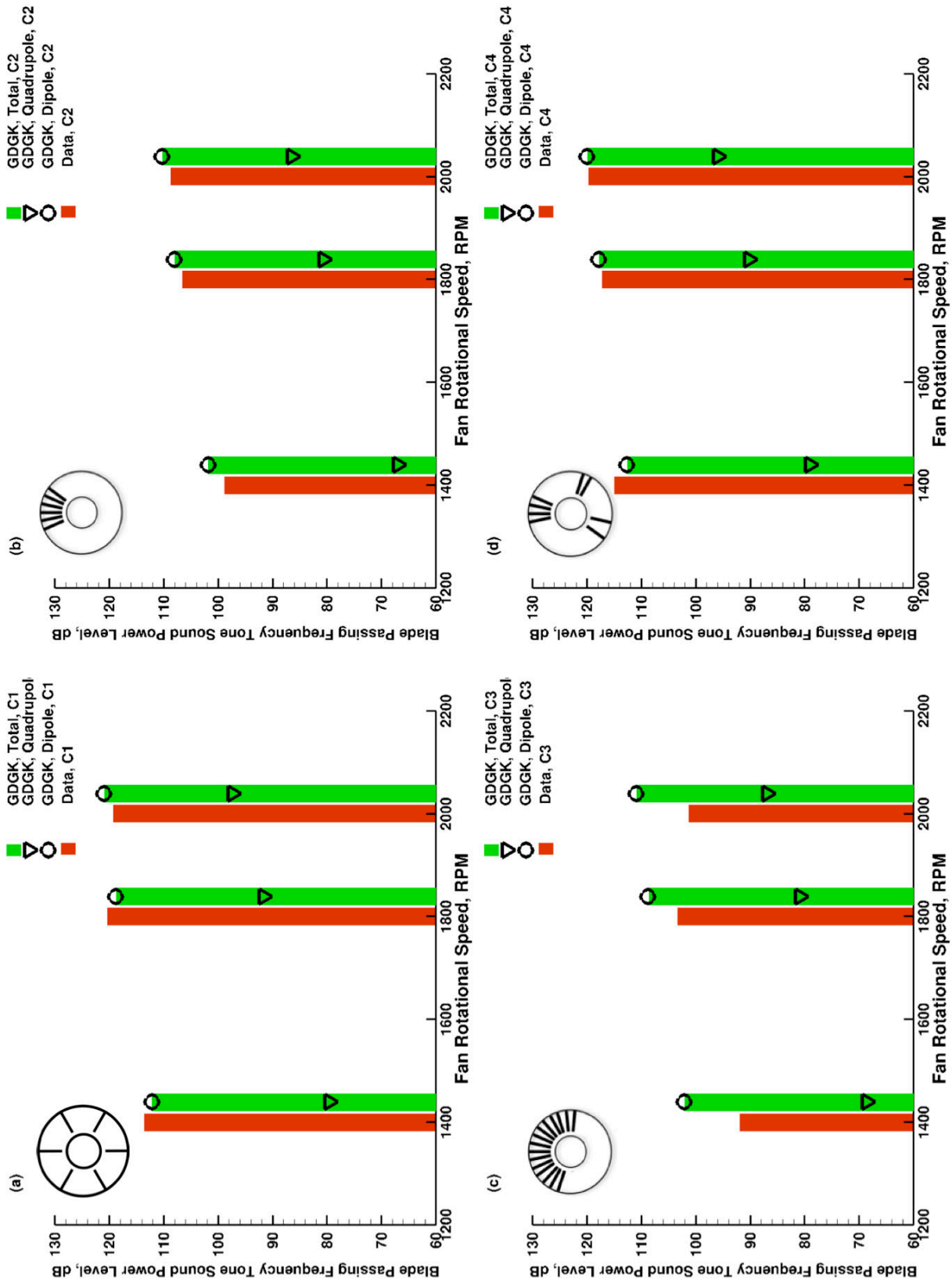


Figure 13.—Calculated ( $P_1$ ) and measured ( $P_1$ ) fundamental tone sound power levels for the inlet region. Symbols represent the sound power levels of the dipole and quadrapole term, while the green bars represent the sound power levels calculated by combining both the quadrapole and dipole terms. Measurements were obtained from the far field microphone array in the inlet region of the ANCF.



REPORT DOCUMENTATION PAGE			Form Approved OMB No. 0704-0188		
<p>The public reporting burden for this collection of information is estimated to average 1 hour per response, including the time for reviewing instructions, searching existing data sources, gathering and maintaining the data needed, and completing and reviewing the collection of information. Send comments regarding this burden estimate or any other aspect of this collection of information, including suggestions for reducing this burden, to Department of Defense, Washington Headquarters Services, Directorate for Information Operations and Reports (0704-0188), 1215 Jefferson Davis Highway, Suite 1204, Arlington, VA 22202-4302. Respondents should be aware that notwithstanding any other provision of law, no person shall be subject to any penalty for failing to comply with a collection of information if it does not display a currently valid OMB control number.</p> <p>PLEASE DO NOT RETURN YOUR FORM TO THE ABOVE ADDRESS.</p>					
1. REPORT DATE (DD-MM-YYYY) 01-09-2012		2. REPORT TYPE Technical Memorandum		3. DATES COVERED (From - To)	
4. TITLE AND SUBTITLE Predicting the Inflow Distortion Tone Noise of the NASA Glenn Advanced Noise Control Fan With a Combined Quadrupole-Dipole Model			5a. CONTRACT NUMBER		
			5b. GRANT NUMBER		
			5c. PROGRAM ELEMENT NUMBER		
6. AUTHOR(S) Koch, L., Danielle			5d. PROJECT NUMBER		
			5e. TASK NUMBER		
			5f. WORK UNIT NUMBER WBS 561581.02.08.03.45.02.04		
7. PERFORMING ORGANIZATION NAME(S) AND ADDRESS(ES) National Aeronautics and Space Administration John H. Glenn Research Center at Lewis Field Cleveland, Ohio 44135-3191			8. PERFORMING ORGANIZATION REPORT NUMBER E-18348		
9. SPONSORING/MONITORING AGENCY NAME(S) AND ADDRESS(ES) National Aeronautics and Space Administration Washington, DC 20546-0001			10. SPONSORING/MONITOR'S ACRONYM(S) NASA		
			11. SPONSORING/MONITORING REPORT NUMBER NASA/TM-2012-217673		
12. DISTRIBUTION/AVAILABILITY STATEMENT Unclassified-Unlimited Subject Categories: 02 and 71 Available electronically at <a href="http://www.sti.nasa.gov">http://www.sti.nasa.gov</a> This publication is available from the NASA Center for AeroSpace Information, 443-757-5802					
13. SUPPLEMENTARY NOTES					
14. ABSTRACT A combined quadrupole-dipole model of fan inflow distortion tone noise has been extended to calculate tone sound power levels generated by obstructions arranged in circumferentially asymmetric locations upstream of a rotor. Trends in calculated sound power level agreed well with measurements from tests conducted in 2007 in the NASA Glenn Advanced Noise Control Fan. Calculated values of sound power levels radiated upstream were demonstrated to be sensitive to the accuracy of the modeled wakes from the cylindrical rods that were placed upstream of the fan to distort the inflow. Results indicate a continued need to obtain accurate aerodynamic predictions and measurements at the fan inlet plane as engineers work towards developing fan inflow distortion tone noise prediction tools.					
15. SUBJECT TERMS Fans; Noise					
16. SECURITY CLASSIFICATION OF:			17. LIMITATION OF ABSTRACT	18. NUMBER OF PAGES 24	19a. NAME OF RESPONSIBLE PERSON STI Help Desk (email:help@sti.nasa.gov)
a. REPORT U	b. ABSTRACT U	c. THIS PAGE U			UU



